DOI: 10.21062/mft.2026.045 © 2026 Manufacturing Technology. All rights reserved. http://www.journalmt.com

Evaluation of Formability of Laser Tailor Welded Blanks

Alexander Schrek (0000-0002-6971-8446), Alena Brusilová (0000-0002-8065-2433), Zuzana Gábrišová (0000-0003-3683-1220), Pavol Švec (0000-0003-4176-1263)
Institute of technologies and materials, Faculty of Mechanical Engineering, STU Bratislava, Nám. Slobody 17, 812 31 Bratislava. Slovakia. E-mail: alexander.schrek@stuba.sk, alena.brusilova@stuba.sk, zuzana.gabrisova@stuba.sk, pavol.svec@stuba.sk

The car body construction is made from workpieces on which specific demands are put. The high stiffness and strength, low weight, programmable deformability is achieved by using of tailored welded blanks (TWBs). The weld joint is most commonly realized by a laser weld with a narrow heat affected zone (HAZ). The formability of TWB is affected by the weld, stress-strain characteristics of materials and process conditions. For the analysis of TWBs, materials with the same thickness, but different orientation of the texture of the individual parts with respect to the position of the weld, were used. The effect of surface anisotropy of individual materials on formability was studied in terms of the origin and direction of crack propagation during deep drawing or tension test. The sensitivity of individual materials to the presence of a weld, the formation of a crack and the course of changes in microhardness in the weld and HAZ was evaluated. The obtained results are important in the design of TWB from the point of view of the presence of a weld and the orientation of the texture of individual parts of the TWB in relation to local limit strains and the risk of cracks formation.

Keywords: deep drawing, tailor welded blank, weld, crack, anisotropy

1 Introduction

Tailor welded blanks consisting of materials with different stress-strain characteristics or different thicknesses are widely used for the parts production of car body construction. The task is to achieve the required stiffness, strength but at the same time the ability to absorb the plastic deformation work during impact with the smallest possible weight Fig. 1,2 [1–3].

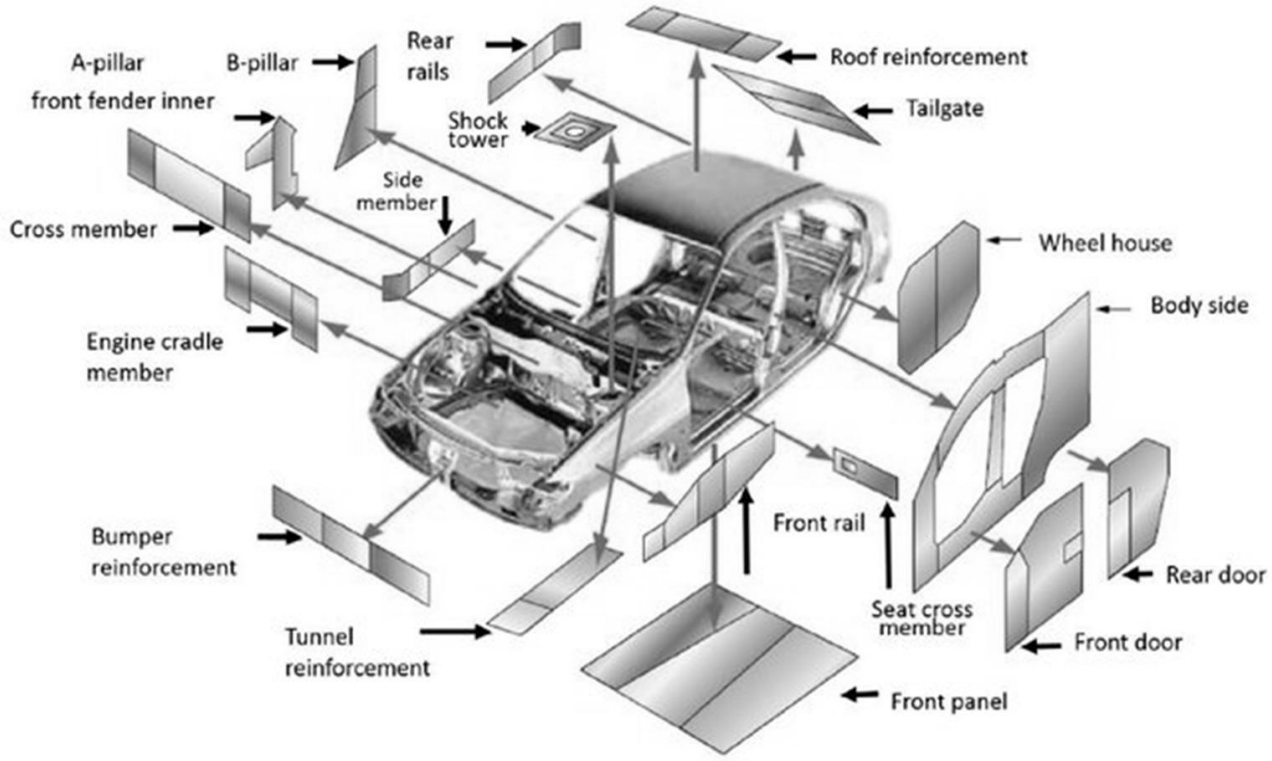


Fig. 1 *The range of TWBs applications in the car body construction [4]*

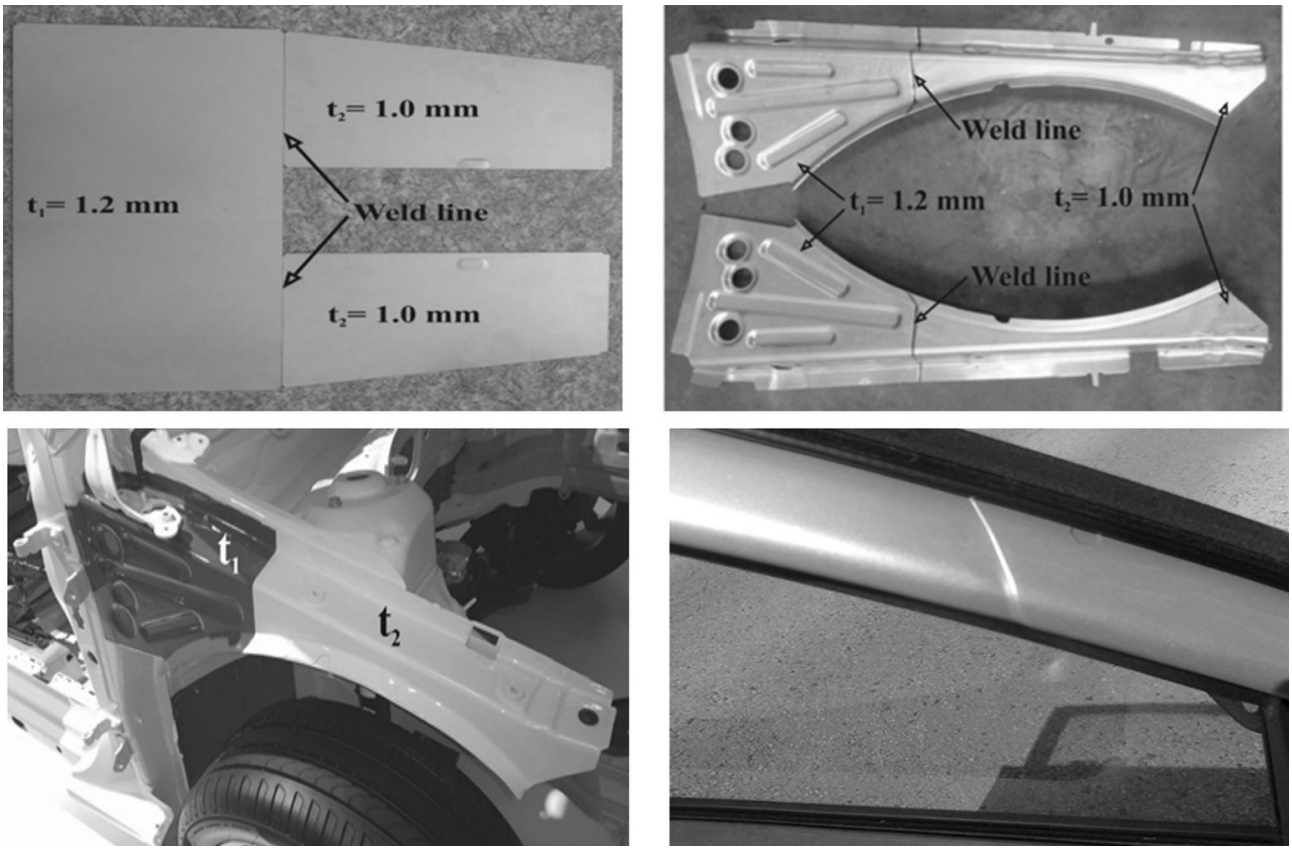


Fig. 2 *Examples of using TWBs*

BH, HSLA, DP-HCT, TRIP steels are among the very often used materials of tailor welded blanks. Structural changes in the heat-affected zone of the weld joint affect their deformation properties and can be a source of cracks formation during the production of workpieces [5]. Connecting individual parts is realized by various methods of welding Figure 3 [2, 3, 6].

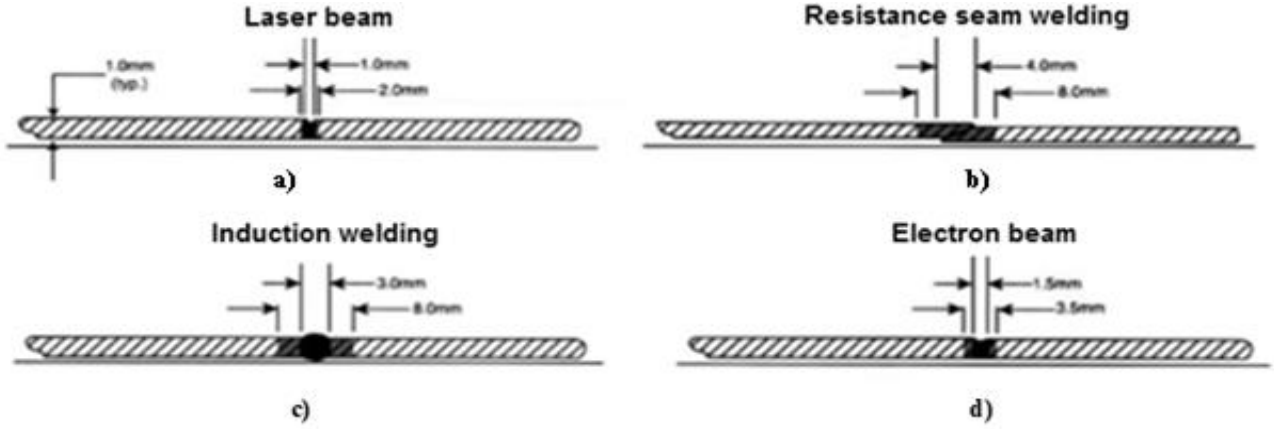


Fig. 3 *Welding of TWBs and comparison of weld width and heat affected zone*

The most common way to formation a joint is laser welding, which generates the narrowest heat-affected zone at the point of joint. An appropriate choice of technological welding conditions (power, welding speed) will make it possible to maintain the deformation properties in the vicinity of the weld joint as close as possible to the base material [7–9]. Nevertheless, the weld joint will negatively affect the formability of the TWB. Many technological tests can be used to evaluate formability - Erichsen's, Gross-Engelhardt's, Deep drawing cup test, Siebel and Pompa's, Fukui's, Tomlen's, FLD-diagram tests which represent a complex idea of the real stress-strain conditions during the forming process and the biaxial stress state [10,11].

The presented results were obtained by investigating the effect of surface anisotropy on the formation of cracks during deep drawing of tailor

welded blanks at the limiting drawing ratio. During the rolling process, a texture is formed, which causes differences in the tension and deformation properties of sheet materials depending on the direction of rolling. However, the sensitivity of individual steels to the production process is different. The aim of the paper was to monitor the sensitivity of steels used in tailor welded blanks with laser weld to the place of origin and the orientation of crack formation with respect to the direction of rolling of individual parts of TWB and the position of the weld. At the same time, the effect of the weld on the change in hardness in the weld and HAZ was also evaluated [7–9, 12].

1.1 Anisotropy of properties

Anisotropy is defined as a phenomenon where material properties change depending on the direction in which we measure these properties. Properties in the direction of rolling are considered to be reference. In polycrystalline metals, the anisotropy is influenced by the chemical composition as well as the oriented macrostructure, i.e. the structural texture that arises after hot rolling. This texture causes the elongation of discontinuities, non-metallic inclusions and regions of different chemical composition in the rolling direction. Another factor is the oriented microstructure, i.e. crystallographic texture, which is formed during cold rolling by the elongation and twisting of plastically deformed crystalline grains in the direction of the most intensive flow of the material. There is crystallographic orientation of grains, inhomogeneities and inclusions and spatial rotation of crystallographic axes in grains in one direction, which are characterized by crystallographic texture. The arrangement of the grains can be random or they can have a certain directional arrangement. Metal crystals will have different stress-strain properties in individual directions [13–17].

1.1.1 Normal anisotropy

Normal anisotropy is characterized by non-uniformity of the material properties in the sheet rolling direction compared to the properties in the direction perpendicular to the sheet plane. It is evaluated as the sheet's resistance to thinning during plastic deformation [18,19].

It is defined by the ratio of the true strain in the width direction to the true strain in the thickness direction in the area of uniform plastic deformation. The expression of normal anisotropy is the coefficient of normal anisotropy *r*:

$$r = \frac{\varphi_b}{\varphi_s} = \frac{\ln \frac{b_0}{b_k}}{\ln \frac{s_0}{s_k}} = \frac{\ln \frac{b_0}{b_k}}{\ln \frac{L_k x b_k}{L_0 x b_0}}, \qquad (1)$$

Where:

φ_b…True strain in the width direction;

φ_s…True strain in the thickness direction.

If r = 1, the tested sheet is isotropic, i.e. the sheet will be deformed equally in the direction of width and thickness during lengthening. If r < 1, the degree of strain in the direction of thickness prevails and the material is prone to thinning of the cross-section of the workpiece wall. If r > 1, the degree of strain in the direction of width and length prevails, the material is more suitable for deep drawing. Smaller thinning of the wall thickness of the workpiece in the area of transmission of the forming force reduces the risk of wall failure [17].

1.1.2 Planar anisotropy

Using the coefficient of normal anisotropy *r* determined in different directions with respect to the direction of rolling (Fig. 4), the planar anisotropy of the mechanical properties can also be determined [17].

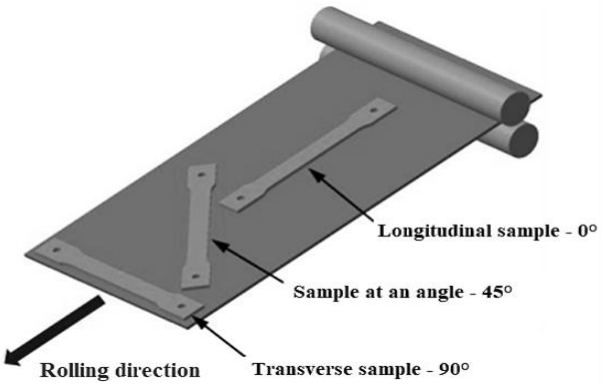


Fig. 4 *Different directions of samples taken with respect to the direction of rolling*

The differences between the values measured in the direction parallel to the rolling direction and the values measured in other directions express the degree of surface anisotropy and the susceptibility to earing formation. The degree of planar anisotropy of the normal anisotropy coefficient ⊿*r* is defined:

$$\Delta r = \frac{1}{2}\left(r_{0^\circ} - 2xr_{45^\circ} + r_{90^\circ}\right) \qquad (2)$$

Planar anisotropy is a consequence of structural and crystallographic deformation, respectively annealed texture, which is associated with metallographic and production conditions. This non-uniformity of the mechanical properties in different directions of the sheet plane is expressed by the planar anisotropy coefficient *a*. It is most often determined for Rm, Re and A.

$$a_{R_e} = \frac{R_{e(\alpha)} - R_{e(0^\circ)}}{R_{e(0^\circ)}} \qquad (3)$$

$$a_{R_m} = \frac{R_{m(\alpha)} - R_{m(0^\circ)}}{R_{m(0^\circ)}} \quad (4)$$

$$a(R_e / R_m) = \frac{(R_e / R_m)_{(\alpha)} - (R_e / R_m)_{(0^\circ)}}{(R_e / R_m)_{(0^\circ)}} \quad (5)$$

$$a_A = \frac{A_{(\alpha)} - A_{(0^\circ)}}{A_{(0^\circ)}} \quad (6)$$

Planar anisotropy is significant in the orientation of the blank in the forming tool. The rolling directions of the sheet metal with the best plastic properties should be identical to the directions of the most difficult strain conditions on the workpiece. Planar anisotropy has a fundamental influence on pressability. The value of the planar anisotropy coefficient should be as small as possible [17].

Another criterion of sheet formability is the mean value of the normal anisotropy coefficient $\bar{r}$:

$$\bar{r} = \frac{1}{4}(r_0 + 2r_{45} + r_{90}) \quad (7)$$

Where:

r_0, r_{45}, r_{90}…The coefficients of normal anisotropy in the direction 0°, 45°, 90° with respect to the sheet rolling direction.

The higher the $\bar{r}$ value and the lower the Δr value, the more resistant the metal sheet is to thinning of thickness and the more suitable it is for deep drawing. According to Shawki, the classification of metal sheets is as follows:

- low formability: $\bar{r} < 1{,}25$
- good formability: $\bar{r} = (1{,}25 - 1{,}60)$
- excellent formability: $\bar{r} > 1{,}60$

In the case of deep drawing of drawn parts with a complex shape, the blanks should be oriented so that the directions of the largest values of the normal anisotropy coefficient are in the places of maximum deformation [9]. The importance of normal anisotropy becomes apparent only in the case of limit strains in exposed areas of drawn parts with a complex shape, when a crack is formed in the case of inappropriately chosen material or inappropriate deep drawing parameters. Compared to planar anisotropy, which is manifested by the earing formation, normal anisotropy isn´t observable in common deformations [9]. In the case of tailored welded blanks and inappropriate rolling orientation of individual parts with significantly different forming properties, planar anisotropy is also manifested by the formation of cracks [17].

2 Materials and Methods

2.1 Material characteristics

2.1.1 Steels hardenable at baking the varnish BH220

They belong to low-carbon steels with a ferritic structure. The chemical composition of the steel is in Tab. 1. They have a low yield strength and high plasticity before pressing. After pressing and baking the varnish, deformation-thermal strengthening occurs in the workpieces, thereby increasing the yield strength by 30–80 MPa. This strengthening is related to the process of deformation aging under heat, which is conditioned by the diffusion of carbon and nitrogen atoms to the dislocations created during pressing. Since the diffusion of carbon atoms in ferrite is considerably lower at ambient temperatures compared to nitrogen, it is convenient to control the aging process by means of thermal activation of carbon atoms. Atoms that were originally dissolved in the deformed ferrite subsequently diffuse into the vicinity of the dislocations during baking the varnish and create a Cottrell atmosphere. Beneficial elements that influence the height of the BH effect in addition to carbon in steel are Mn, Si and P.

BH steels are mainly used for large-scale workpieces of body parts - roofs, hoods and doors. After pressing and baking the varnish, the maximum permissible load and resistance to indentation increases. Due to the low content of basic and alloying elements, BH steels have good weldability by all conventional welding methods [20]. Mechanical properties can be found in Tab. 2.

Tab. 1 *Chemical compositions (wt. %)$_{max}$ of the BH220 steel*

C	Mn	P	S	Al	Si	N	Nb
0.038	0.20	0.054	0.012	0.051	0.27	0.006	0.09

Tab. 2 *Mechanical properties of BH220 steel*

$R_{p0,2}$ (MPa)	R_m (MPa)	A_{min} (%)	r	a
420-280	320 – 440	31	< 1.5	< 0.25

2.1.2 IF – Interstitial Free steel - HX220 LAD

The structure of these steels is formed of fully ferrite. Their properties are controlled by the size of the ferritic grain, influenced by the microalloying of Ti and Nb. They have extremely high ductility and low yield strength. During the crystallization of these steels, no interstitial atoms are present in the structure that could strengthen the steel. They are mainly intended for deep drawing. They are characterized by a high coefficient of normal anisotropy r and strain hardening exponent n. Thanks to their high resistance to aging, they are suitable for continuous hot-dip galvanization. The chemical composition of the steel is in Tab. 3.

IF steels are intended for deep drawing of complex body parts. They aren´t suitable for strength parts. Fusion and pressure welding methods are used to join parts [21]. The stress-strain parameters of HX220 steel are in Tab. 4.

Tab. 3 *Chemical compositions (wt. %)$_{max}$ of HX 220 LAD steel*

C	Mn	P	S	Si	Al	Ti	Nb
0.01	0.08	0.08	0.025	0.20	0.10	0.12	0.09

Tab. 4 *Mechanical properties of HX 220 LAD steel*

$R_{p0,2}$ (MPa)	R_m (MPa)	A_{min} (%)	r_{90}	a	n_{90}
220-280	340-420	32	< 1.20	< 0.22	0.15

2.1.3 DP - Duplex steels - HCT600 X

DP steels are characterized by high strength and plasticity. Heat treatment in the area of ferrite and austenite by intercritical annealing just below the Ac3 temperature or by controlled rolling and subsequent cooling produces a structure consisting of ferrite (70–80)% and austenite (20–30)%. After subsequent cooling, austenite transforms into martensite. The resulting structure is formed by a soft ferritic matrix affecting formability, in which martensitic formations are dispersed in the form of strength-increasing islands. A suitable structure for cold forming consists of 75–85% ferrite and 15–25% martensite. These steels have excellent resistance to the initiation and propagation of fatigue cracks, good weldability and a high ability to absorb impact energy. They are suitable for strength parts and reinforcements [22-26]. Two-phase steel HCT600 X were used for the analysis. The chemical composition of the steel can be found in Tab. 5, mechanical properties in Tab. 6.

Tab. 5 *Chemical compositions (wt. %)$_{max}$ of HCT600 X steel*

C	Si	Mn	Al	Cr+Mo	Nb+Ti	V	B	P	S
0.17	0.8	2.2	2.0	1.0	0.15	0.2	0.005	0.08	0.015

Tab. 6 *Mechanical properties of HCT600 X steel*

$R_{p0,2}$ (MPa)	R_m (MPa)	A_{min} (%)	r	a
340-420	min 600	20	< 0.9	< 0.1

2.2 Methods

2.2.1 Preparation of samples

TWB samples were welded with a solid-state Nd:YAG laser marked ROFIN-DY 044 using the SCANSONIC-ALO 3 adaptive welding head, which is part of the KUKA robotic arm. The power of the laser beam was 2200 W and 2400 W depending on the thickness of the sheet. The welding speed was constant for all samples at 40 mm.s^{-1}, focusing f = 6 mm.

2.2.2 Biaxial tensile test

The test was performed on a double-acting hydraulic press PYB 160 S, with a nominal force of 1600 kN. The test sample with dimensions of 180 x 180 mm was clamped between the die and the blank holder with the maximum holding force of the lower ram of 320 kN, the holding pressure was 11 MPa. This prevented the material from being pulled out from under the blank holder into the die and the blank was stretched. The hemispherical punch had a diameter of 60 mm. The ram movement speed was 5 mm.s^{-1}. The sample was stretched until the crack started to propagate. The Erichsen index (IE) was not evaluated during the test. The samples were analyzed from the point of view of the place of origin and the orientation of the crack propagation with respect to the orientation of the rolling direction of individual parts of the tailor welded blank. The model of the experimental and test tool and its application on the forming machine during the test is in Figure 5.

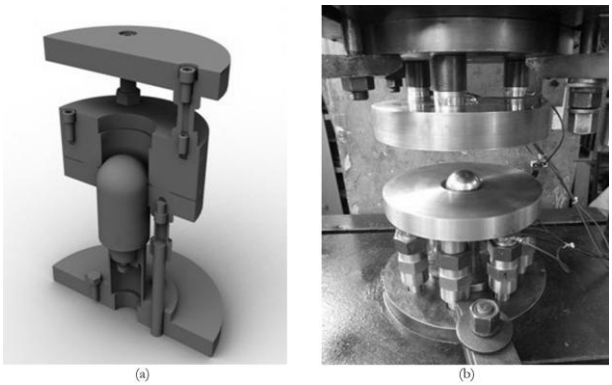


Fig. 5 *a) Test tool model, b) Tool fixed in the PYB160S machine*

2.2.3 Measurement of microhardness

To measure the microhardness, samples were taken from the weld joint of the tailor welded blanks. Transverse cross-sectons of the welds were prepared for evaluation by standard metallographic procedures by grinding, polishing, and etching with a 1% Nital solution. The hardness measurement zone in the weld and its surroundings had a length of at least 4 mm and made it possible to obtain an overview of changes in the base material and the weld joint. Microhardness on transverse cross-sectons was measured using the Vickers method with a load of 100 g. Buehler Indenta Met 1100 with Omni Met HMS software was used to measure impressions dimensions and evaluate microhardness. From the measured values, courses of microhardness in welded joints were made.

3 Results

For the experiments, samples were prepared from selected materials used for workpieces of load-bearing parts - skeleton, as well as surface parts of car bodies. Blanks from one material were welded from parts with different orientations of rolling directions. After deep-drawing process, the places where the crack appeared, its orientation and the direction of propagation with respect to the position of the weld and the direction of rolling were monitored and compared. The sensitivity of individual steels to the presence of a weld and different orientation of the rolling direction was compared. The photos of the details of individual samples is marked the type of steel, sheet thickness, welding parameters: power, speed, focusing and the orientation of the rolling direction of the parts of the workpiece indicated by arrows.

3.1 BH220 steel

In a sample where both parts of the blank have the same orientation in the rolling direction with the weld, a crack formed in the weld at the point of increased hardness and reduced cross-section and propagated along the contour line (Fig. 6). This configuration of the blank is sensitive to the presence of a weld.

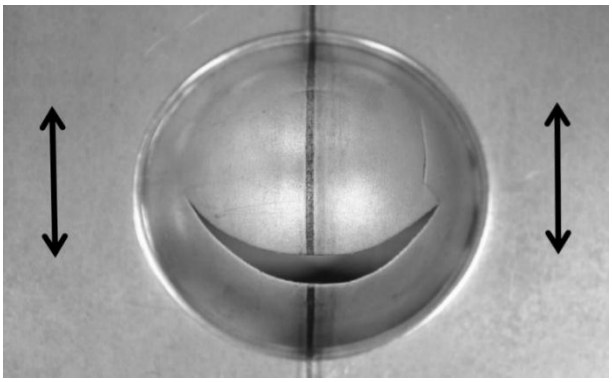


Fig. 6 *Detail of a crack on the sample BH 220; 1.2 mm, 2200/40/f+6*

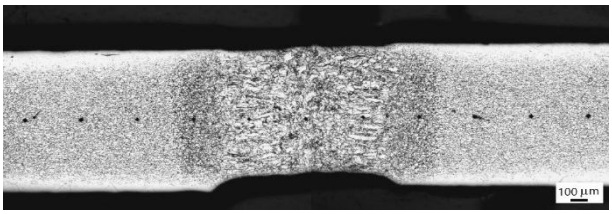


Fig. 7 *Transverse cross-section of the weld, material BH220*

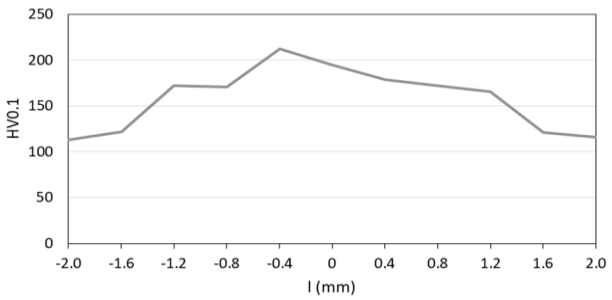


Fig. 8 *Course of microhardness, material BH220*

From Fig. 7 and 8 it can be seen that the hardness in the weld and in the heat affected zone increased from 113 HV0.1 to 212 HV0.1, which is an 87.6% increase. With a significant reduction in plasticity, the crack began to propagate in the weld. Another reason was the reduced cross-section in this place (Fig. 7). The weld and heat-affected zone measures approx. 3.2 mm.

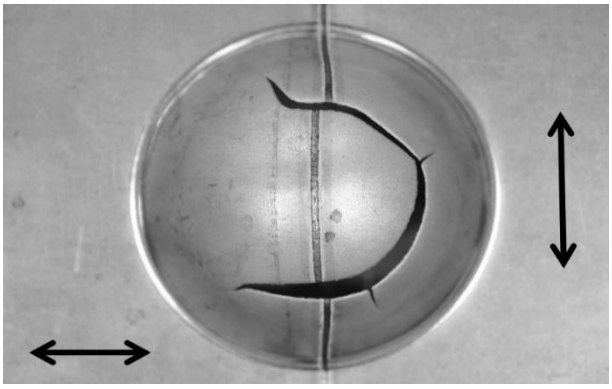


Fig. 9 *Detail of a crack on the sample BH220; 1.2 mm, 2200/40/f+6*

Fig. 9 shows a sample with a combined rolling direction of individual parts – along and perpendicular to the weld. The crack started to propagate outside the weld joint, then propagated along the contour line. The crack was initiated on the part of the sample that had the rolling direction parallel to the weld at the point of increased hardness. It follows that the weld in this sample had no effect on the formation and propagation of the crack.

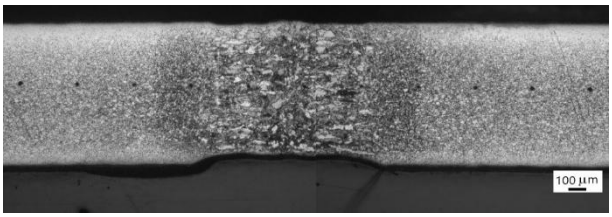


Fig. 10 *Transverse cross-section of the weld, material BH220*

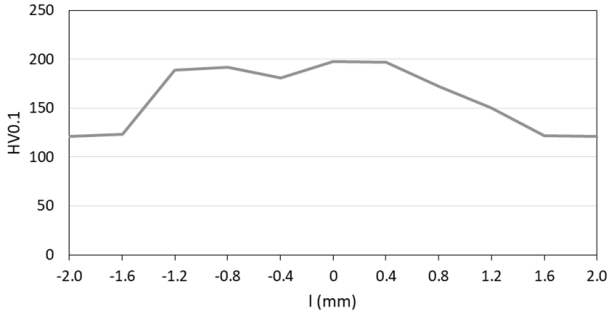


Fig. 11 *Course of microhardness, material BH220*

In Fig. 10 is a weld with a narrowed cross-section and a heat-affected area measuring approx. 3.2 mm. From Fig. 19 we can read the change in hardness in the weld and in the heat-affected zone, which changed from 121 HV0.1 to 198 HV0.1, which represents an increase in hardness by 63.6%.

3.2 HX 220 steel LAD

On the sample (Fig. 12), after the plasticity of the material was exhausted, the crack was initiated in the heat-affected zone of the weld and continued to spread along the contour line. In the cross-section of the weld (Fig. 13), a slight displacement of parts of the tailor welded blanks and a slight change in the cross-section can be observed, which may act as a notch during the transmission of deep-drawing force. The heat affected zone was 3.6 mm wide. In the weld joint, the hardness increased from 140 HV0.1 to 176 HV0.1. Fig. 14 shows an increase in hardness by 25.7%.

On the sample (Fig. 15), after the plasticity of the material was exhausted, the crack initiated at the point where the rolling direction is parallel to the weld and continued to spread along the contour line. In the part of the blank where the rolling direction is perpendicular to the rolling direction, the crack started to change direction in its final stage of propagation. In the cross-section of the weld (Fig. 16), a small thinning of the cross-section can be observed, which may act as a notch during the transmission of deep-drawing force. The heat affected zone measures 3.6 mm. In the weld joint, the hardness increased from 136 HV0.1 to 169 HV0.1 Fig. 17 shows an increase in hardness by 24.3%.

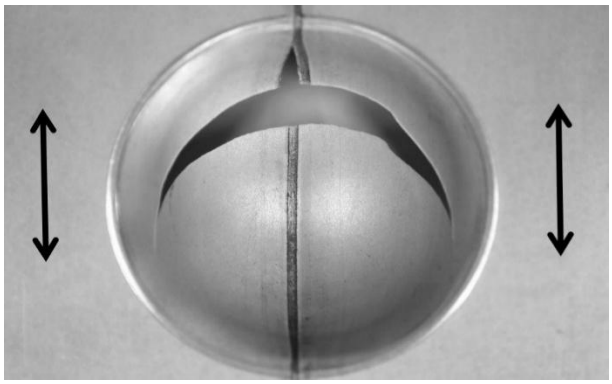


Fig. 12 *Detail of a crack on the sample HX220 LAD; 0.8 mm, 2200/40/f+6*

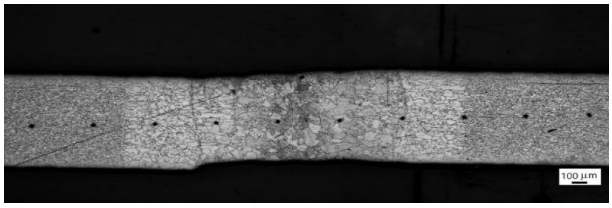


Fig. 13 *Transverse cross-section of the weld, material HX220 LAD*

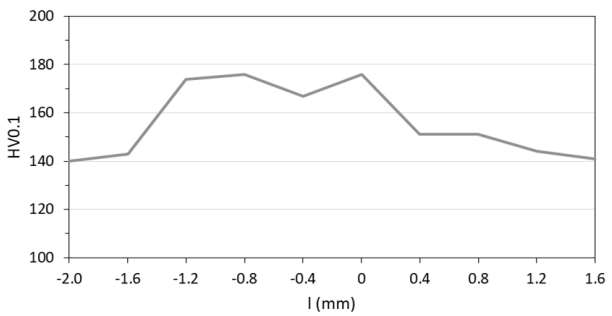


Fig. 14 *Course of microhardness HV0.1 of the weld joint, steel HX220 LAD*

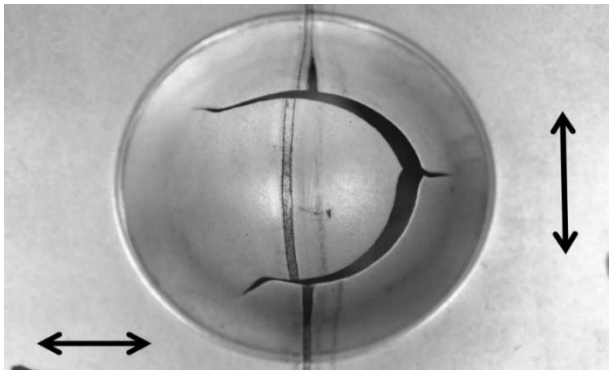


Fig. 15 *Detail of a crack on the sample HX220 LAD; 0.8 mm, 2200/40/f+6*

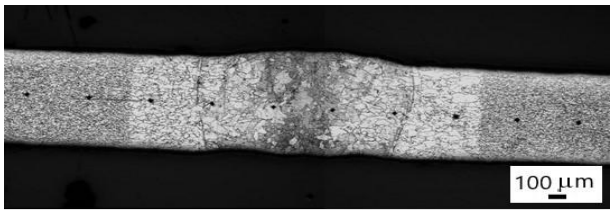


Fig. 16 *Transverse cross-section of the weld, material HX220 LAD*

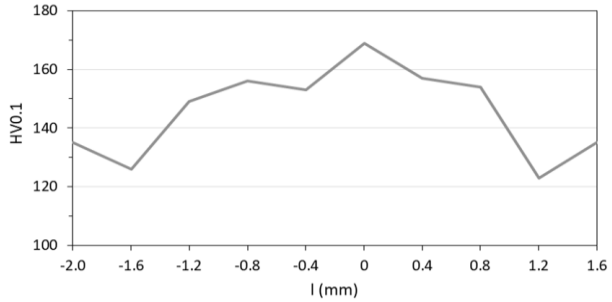


Fig. 17 *Course of microhardness HV0.1 of the weld joint, steel HX220 LAD*

3.3 Steel HCT600 X

In Figure 18, it can be observed that the crack was initiated in the weld and then propagated along the contour line. It follows that the sample with a combined rolling direction of the individual parts – along and perpendicular to the rolling direction – is sensitive to the presence of the weld. The heat-affected zone measures 3.2 mm (Fig. 19). Figure 20 shows the course of the hardness change, which increased from 228 HV0.1 to 387 HV0.1, which represents an increase in hardness by 70%.

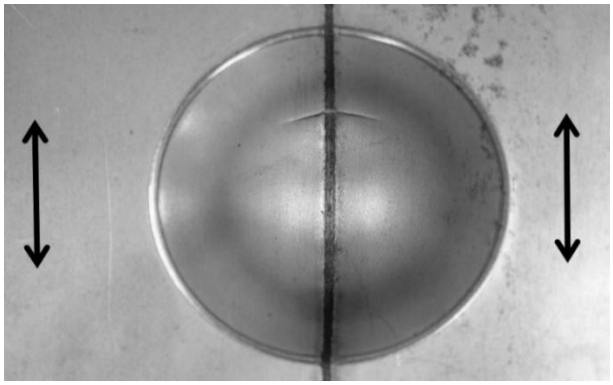


Fig. 18 *Detail of a crack on the sample HCT600 X; 1.2 mm, 2400/40/f+6*

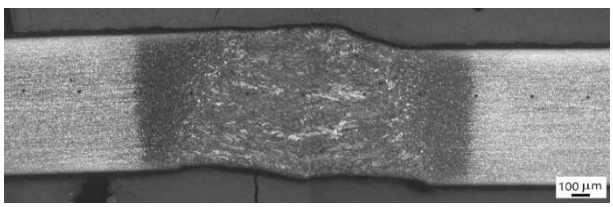


Fig. 19 *Transverse cross-section of the weld, material HCT600 X*

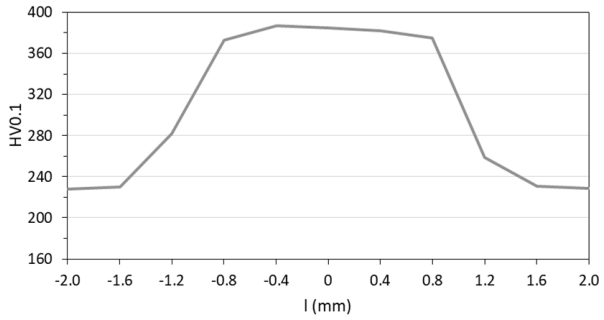


Fig. 20 *Course of microhardness HV0.1 of the weld joint, steel HCT600 X*

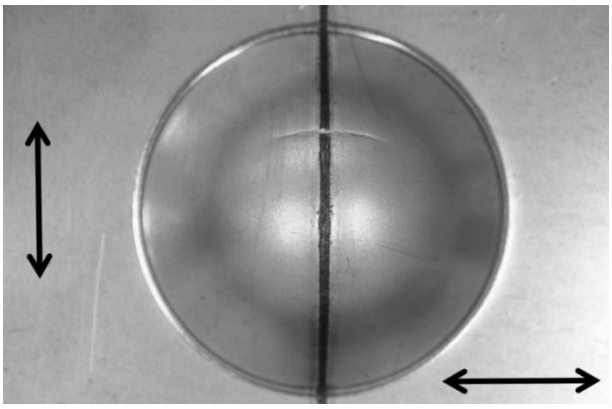


Fig. 21 *Detail of a crack on the sample HCT600 X; 1.2 mm, 2400/40/f+6*

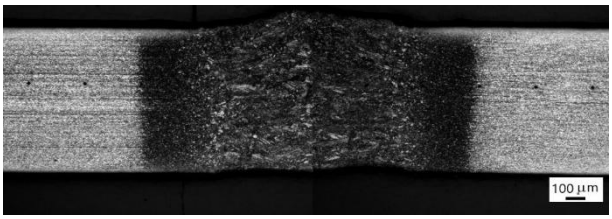


Fig. 22 *Transverse cross-section of the weld, material HCT600 X*

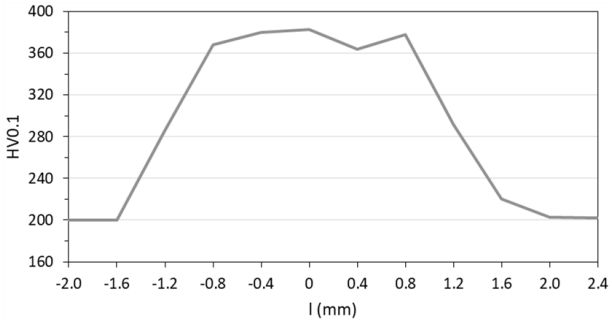


Fig. 23 *Course of microhardness HV0.1 of the weld joint, steel HCT600 X*

As seen in Figure 21, the crack started to propagate in the weld and continued to propagate along the contour line. It follows that this material is sensitive to the presence of a weld. Since the sample consists of sheets with different rolling directions and the crack propagates in both directions, it can be concluded that

this material isn´t sensitive to planar anisotropy. The heat-affected zone measures 3.2 mm (Fig. 22). Figure 23 shows an increase in hardness from 200 HV0.1 to 383 HV0.1, which represents an increase of 91.5%.

4 Discussion

When joining two sheets of the same material and thickness, uniaxial loading perpendicular to the weld may cause failure in the weld, in the heat-affected zone, or in the base material. During indentation with a hemispherical punch, a biaxial stress state is created in the material. Welded sheets with different planar and normal anisotropy behave differently under extreme deformation. It was found that at high values of planar anisotropy (a >0.5) and low values of normal anisotropy (r <1), in the case of the same (longitudinal) orientation of the rolling direction of the sheets with the weld, the crack primarily originates in the weld and propagates along the weld. In the case of a combined orientation of the rolling direction of the sheets (perpendicular and longitudinal) with the weld, the crack occurs on the side of the sheet with the longitudinal rolling direction. Sheet metal with a rolling direction perpendicular to the weld offers greater resistance to crack formation and propagation. The heat-affected zone is narrow, but the steep temperature gradient contributes to the formation of internal stresses and brittle phases of martensite and bainite [27,28].

Based on the above experimental results, the following conclusions can be drawn:

- Steel BH220 – average normal anisotropy r = 1.5, planar anisotropy a < 0.25 - the crack was formed in an unsupported area by a punch and a die on the side of the blank where the rolling direction was parallel to the weld. The second side of the blank had the rolling direction perpendicular to the weld. In the case of the same (longitudinal) orientation of the rolling direction of the blank with the weld, the crack originated in the weld and propagated along the contour line. Crack initiation could have been influenced by the formation of acicular ferrite and bainite and grain coarsening in the weld [27,28]. The increase in microhardness in the weld represented an increase of 87.6%. Steel, due to the higher value of the planar anisotropy coefficient, will not be sensitive to the presence of a weld, but will be sensitive to planar anisotropy.
- Steel HX220 LAD – average normal anisotropy r = 1.2, planar anisotropy a < 0.22 - the crack was formed in an unsupported area by a punch and a die on the side of the blank where the rolling direction was parallel to the weld. The second side of the blank had the rolling direction perpendicular to the weld. In the case of the same (longitudinal) orientation of the rolling direction of the blank with the weld, the crack originated in the weld and propagated along the contour line. Crack initiation could have been influenced by the formation of larger Ti and Nb precipitates in the weld and grain coarsening, which reduce plasticity [29]. The increase in microhardness in the weld represented an increase of 25.7%. The formation and propagation of the crack was influenced by the rolling direction of the individual parts of the blank and the higher value of the planar anisotropy coefficient. Steel will not be sensitive to the presence of a weld, but will be sensitive to planar anisotropy.
- Steel HCT600 X- average normal anisotropy r = 0.9, planar anisotropy a < 0.1 - the crack initiated in the weld and propagated along the contour line, regardless of the rolling direction. The weld structure is made up of martensite and bainite with significantly lower plasticity. Intense residual tensile stresses also arise in the center of the weld, close to the yield point of the base material [28,30]. The increase in microhardness in the weld represented an increase of 91.5%. Steel will not be sensitive to planar anisotropy, but it will be sensitive to the presence of a weld.

5 Conclusions

The aim of the research was to evaluate the influence of planar and normal anisotropy on the formability of tailor welded blanks (TWBs). The obtained results are important for the design of TWBs from the point of view of the presence of the weld and the rolling orientation of individual parts in relation to the direction of principal stresses, to local limit strains and the risk of cracks in exposed areas of deep-drawn parts. Three types of steels were

evaluated, bake hardening BH220; micro-alloyed HX220LAD and dual-phase HCT600, which are used in the construction of passenger car bodies. The presented results represent a prediction of their suitability for use. Based on the obtained results, the tested steels can be divided into 3 groups:

- 1. TWBs (BH220): BH220 are steels where, when the rolling directions of the individual parts of the TWB are oriented in the same rolling direction, a crack forms in the weld. When the rolling direction is different (parallel and perpendicular to the weld), the crack occurs at the point of greatest tensile stress. The crack propagates symmetrically along the contour, passes through the weld and continues on the side of the TWB that has the rolling direction perpendicular to the weld.
- 2. TWBs (HX220LAD): HX220LAD are steels where, when the rolling directions of the individual parts of the TWB are oriented in the same rolling direction, a crack forms in the weld. With different orientations of the rolling direction (parallel and perpendicular to the weld), the crack occurs at the point of greatest tensile stress. The crack propagates symmetrically along the contour line to the weld and continues to the side of the TWB that has the rolling direction perpendicular to the weld.
- 3. TWBs (HCT600 X): HCT600 X are steels sensitive to the presence of weld, where a crack originates in the weld or in the heat-affected zone and propagates along the contour line, regardless of the orientation of the rolling direction of the individual parts of the TWB and the direction of stress application. Due to the very low planar anisotropy, the steel is not sensitive to the orientation of the rolling direction. Crack propagation is influenced by the low coefficient of normal anisotropy and structural changes in the weld, which reduce the plasticity of the material.

In the case of deep drawing of body parts with complex shapes, the location of the weld of the TWB should be outside the places with limit strains. The orientation of the rolling direction of the individual parts of the TWB should be parallel to the direction of the greatest stresses that arise during deep drawing process. In the case of large local strains of drawn parts, steels with the highest values of the normal anisotropy coefficient and values of the planar anisotropy coefficient approaching zero are suitable, which reduces the risk of cracks in these places.

Acknowledgement

This work was supported by the University Science Park STU Bratislava ITMS code 26240220084. We would like to thank the Slovak grant agency VEGA for the financial support of the project VEGA 1/0302/23.

References

[1] EVIN, E., TOMÁŠ, M. (2012). Comparison of deformation properties of steel sheets for car body parts. In: *Procedia Engineering,* Vol. 48, pp.115–122.

[2] EVIN, E. (2013). Design of dual phase high strength steels sheet for auto body. In: *22nd International Conference on Metallurgy and Materials – METAL 2013*. Ostrava: Tanger.

[3] HRIVŇÁK, A., EVIN, E. (2004). *Formability of Steel Sheets, 1st ed.*; Alfa: Košice, Slovakia.

[4] www.arcelormittal.com

[5] MEŠKO, J., ZRAK, A., MULCZYK, K., TOFIL, S. (2014). Microstructure Analysis of Welded Joints after Laser Welding. In: *Manufacturing Technology*, Vol. 14, No. 3, pp. 355-359.

[6] EVIN, E., TOMÁŠ, T. (2017). The Influence of Laser Welding on the Mechanical Properties of Dual Phase and Trip Steels, In: *Metals,* Vol. 7, p. 239.

[7] MERKLEIN, M., JOHANNES, M., LECHNER, M., KUPPERT, A. (2014). A review on tailored blanks - Production, applications and evaluation. In: *J. Mater. Process. Technol.*, Vol. 214, pp. 151–164.

[8] PODANY, P., REARDON, C., KOUKOLIKOVA, M., PROCHAZKA, R., FRANC, A. (2018). Microstructure, Mechanical Properties and Welding of Low Carbon, Medium Manganese TWIP/TRIP Steel. In: *Metals*, Vol. 8, p. 263

[9] XIE, J., MA, Y., OU, M., XING, W., ZHANG, L., LIU, K. (2018). Evaluating the Microstructures and Mechanical Properties of Dissimilar Metal Joints Between a New Cast Superalloy K4750 and Hastelloy X Alloy by Using Different Filler Materials. In: *Materials,* Vol. 11, p. 2065.

[10] VILLALOBOS, J.C., DEL-POZO, A., CAMPILLO, B., MAYEN, J., SERNA, S. (2018). Microalloyed Steels through History until 2018: Review of Chemical Composition, Processing and Hydrogen Service. *Metals,* Vol. 8, p. 351.

[11] KOREČEK, D., SOLFONK, P., SOBOTKA, J. (2023). Utilization of Metal Forming Process Mathematical Modelling to Predict the Spring-back of the Dual-phase Steel Stamping. In: *Manufacturing Technology*, Vol. 23, No. 6, pp. 827-836.

[12] GAUTAM, V., KUMAR, A. (2019). Experimental and Numerical Studies on Formability of Tailor Welded Blanks of High Strength Steel. In: *Procedia Manuf.*, Vol. 29, pp. 472–480.

[13] MUJICA, L., WEBER, S., PINTO, H., THOMY, C., VOLLERTSEN, F. (2010). Microstructure and mechanical properties of laser-welded joints of TWIP and TRIP steels. In: *Mater. Sci. Eng.* A, Vol. 527, pp. 2071–2078.

[14] ZDRAVECKÁ, E., SLOTA, J. (2019). Mechanical and Microstructural Investigations of the Laser Welding of Different Zinc-Coated Steels. *Metals*, Vol. 9, p. 91.

[15] DOU, S., WANG, X., XIA, J., WILSON, L. (2020). Analysis of Sheet Metal Forming (Warm Stamping Process): A Study of the Variable Friction Coefficient on 6111 Aluminum Alloy. In: *Metals,* Vol.10, 1189.

[16] PANDA, S.K., RAVI KUMAR, D. (2010). Experimental and numerical studies on the forming behavior of tailor welded steel sheets in biaxial stretch forming. In: *Mater. Des.*, Vol. 31, pp. 1365–1383.

[17] ČADA, R. (2001). Formability of steel sheets. 346 s. REPRONIS, Ostrava. ISBN 80-86122-77-8

[18] SOBOTKA, J., BRADÁČ, J. (2019). Measurement of the Anisotropy Coefficient Development in Dependence on Deformation. In: *Manufacturing Technology*, Vol. 19, No. 4, pp. 692-699.

[19] ŘIHÁČEK, J., PODANÝ, K., FALTÝNEK, F. (2019). Prediction of the Stamped Part Thinning Depending on Its Geometry and Blank Material. In: *Manufacturing Technology*, Vol. 19, No. 2, pp. 314-320.

[20] SAFDARIAN, K. R., MOSLEMI N. H., TORKAMANY, M.J., LIAGHAT, G. (2013). Experimental and theoretical investigation of thickness ratio effect on the formability of tailor welded blank. In: *Opt. Laser. Technol.*, Vol. 51, pp. 24–31.

[21] PANDRE, S., KOTKUNDE, N., TAKALKAR, P., MORCHHALE, A., SUJITH R., SINGH K.S. (2019). Flow stress behavior, constitutive modeling, and microstructural characteristics of DP 590 steel at elevated temperatures. In: *J. Mater Eng Perform.*, Vol. 28, pp. 7565–7581.

[22] CHOI, S. H., KIM, E. Y., WOO, W., HAN, S. H., KWAK, J. H. (2013). The efect of crystallographic orientation on the micromechanical deformation and failure behaviors of DP980 steel during uniaxial tension. In: *Int J Plast*, Vol. 45, pp. 85–102.

[23] SCHREK, A., ŠVEC, P., BRUSILOVÁ, A. (2014). Formability of Tailor-Welded Blanks From Dual-Phase and Bake-Hardened Steels with a Planar Anisotropy Influence. In: *Strength of Materials*, Vol. 49, pp. 550-554.

[24] SONG, Y., HUA, L. (2014). Influences of thickness ratio of base sheets on formability of Tailor Welded Blanks. In: *Procedia Eng.*, Vol. 81, pp. 730–735.

[25] PANDRE, S., TAKALKAR, P., MORCHHALE, A., KOTKUNDE, N., SINGH, K. S. (2020). Prediction capability of anisotropic yielding behaviour for DP590 steel at elevated temperatures. In: *Adv Mater Process Technol*, Vol. 6, No. 2, pp. 396–404.

[26] KOREČEK, D., SOLFRONK, P., SOBOTKA, J. (2022). Analysis of the Dual-phase Steel DP500 Stress-strain Characteristics During the Plane Shear Test. In: *Manufacturing Technology*, Vol. 22, pp. 34-38.

[27] ŠVEC, P., CSICSÓ, T., SCHREK, A., BRUSILOVÁ, A. (2016). Zváranie tenkých plechov z ocelí HCT980X a HX220BD pevnolátkovým vláknovým laserom. In: *Zváranie 2016 [elektronický zdroj] : 44. medzinárodná konferencia, Tatranská Lomnica, 9.-11. november 2016. Zborník*. 1. vyd. Bratislava : Slovenská zváračská spoločnosť, pp. 166-174. ISBN 978-80-89296-19-4.

[28] CSICSÓ, T., ŠVEC, P., SCHREK, A., GÁBRIŠOVÁ, Z. (2016). Štruktúra laserových zvarových spojov z ocelí HCT 600X, HCT980X a HX220BD. In *Zváranie 2016 [elektronický zdroj] : 44. medzinárodná konferencia, Tatranská Lomnica, 9.-11. november 2016. Zborník*. 1. vyd. Bratislava : Slovenská zváračská spoločnosť.

[29] SCHREK, A., ŠVEC, P., BRUSILOVÁ, A. (2017). Formability of Tailor-Welded Blanks From Dual-Phase and Bake-Hardened Steels with a Planar Anisotropy Influence. In *Strength of Materials*. Vol. 49, No. 4, pp. 550-554.

[30] ŠVEC, P., SCHREK, A., HRNČIAR, V., CSICSÓ, T. (2015). Fibre laser welding of dual phase steels. In *Acta Metallurgica Slovaca*. Vol. 21, N o. 4, pp. 311-320. ISSN 1335-1532.